

The Astrophysics of Cataclysmic Variables and Related Objects
ASP Conference Series, Vol. ???, 2005
J.M. Hameury & J.P. Lasota, eds.

The Structure and Origin of Magnetic Fields on Accreting White Dwarfs

K. Reinsch¹, F. Euchner¹, K. Beuermann¹, S. Jordan², and
 B. T. Gänsicke³

¹ *Univ.-Sternwarte, Geismarlandstr. 11, 37083 Göttingen, Germany*

² *Astronomisches Rechen-Institut, 69120 Heidelberg, Germany*

³ *Department of Physics, Univ. of Warwick, Coventry CV4 7AL, UK*

Abstract. We have started a systematic study of the field topologies of magnetic single and accreting white dwarfs using Zeeman tomography. Here we report on our analysis of phase-resolved flux and circular polarization spectra of the magnetic cataclysmic variables BL Hyi and MR Ser obtained with FORS1 at the ESO VLT. For both systems we find that the field topologies are more complex than a dipole or an offset dipole and require at least multipole expansions up to order $l = 3$ to adequately describe the observed Zeeman features and their variations with rotational phase. Overall our model fits are in excellent agreement with observations. Remaining residuals indicate that the field topologies might even be more complex. It is, however, assuring that the global characteristics of our solutions are consistent with the average effective field strengths and the halo field strengths derived from intensity spectra in the past.

1. Introduction

Magnetism at a detectable level is a common phenomenon among white dwarfs. According to recent studies the incidence of objects with surface field strengths exceeding 2 MG is at least $\sim 10\%$ of all single white dwarfs, and could even be higher (Liebert et al. 2003). A similar fraction of $\sim 20\%$ magnetic systems has been found among accreting white dwarfs in cataclysmic variables (Gänsicke, this volume). Observed field strengths range from ~ 1 kG–1000 MG with a peak around 16 MG in single white dwarfs (Wickramasinghe & Ferrario 2000, Gänsicke et al. 2002, Schmidt et al. 2003) and 7–230 MG in magnetic CVs (Beuermann 1998). The frequency distributions of field strengths for both populations are compared in Fig. 1.

The origin of the magnetic fields is not well understood. While it is reasonable to assume that the white dwarfs with the highest magnetic fields evolve from main-sequence Ap and Bp stars, low- and moderate-field magnetic white dwarfs appear to imply another origin. The decay times of the lowest multipole components are predicted to be long compared to the evolutionary ages of the white dwarfs. The magnetic field topologies, at least of isolated white dwarfs, are, therefore, likely to be relics of previous evolutionary phases. In accreting systems, the field structure in the outer layers of the white dwarf, however, may have been significantly changed if the accretion rate is high enough that accretion occurs more rapidly than ohmic diffusion (Cumming 2002) and Rayleigh-Taylor instabilities (Romani 1990).

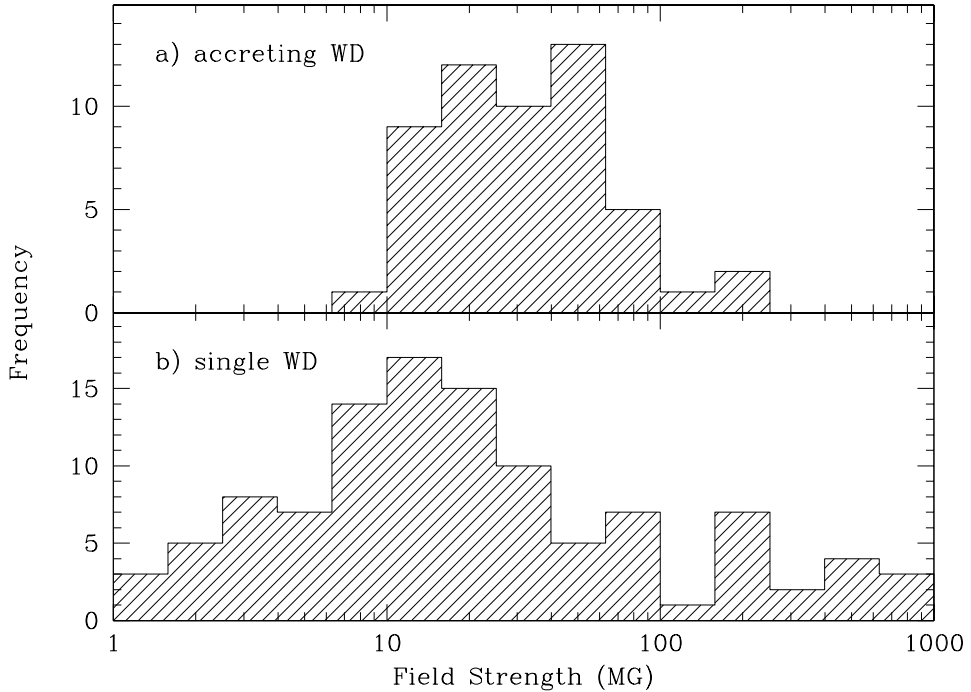


Figure 1. Frequency distributions of the field strengths of accreting (*top*) and single (*bottom*) white dwarfs. For the former, average field strengths in the main accretion region have been used of all 53 polars for which reliable measurements are available (cf. Beuermann 1998). The statistics for single white dwarfs include data from the compilation by Wickramasinghe & Ferrario (2000) and white dwarfs from the SDSS (Schmidt *et al.* 2003). The distribution for magnetic CVs is biased by the omission of low-field systems (intermediate polars) for which only field strength estimates exist and probably also by selection effects which hamper the discovery of high-field polars.

2. Zeeman tomography

Zeeman tomography is a systematic method which we have developed to derive the surface magnetic field structure on rotating white dwarfs (Euchner *et al.* 2002). It utilizes a least-squares optimization code based on an evolutionary strategy to reconstruct the multipole parameters of the field from a series of flux and circular polarization spectra obtained at different rotational phases. The observational data are fitted with a database of precomputed Zeeman spectra of homogeneous magnetic white dwarf atmospheres calculated with a code developed by S. Jordan for a grid of field strengths B , effective temperatures T , and angles ψ between the field direction and the line of sight.

3. Observations

Within our framework of systematic field topology studies of single and accreting magnetic white dwarfs we have obtained spin-phase resolved circular spectropo-

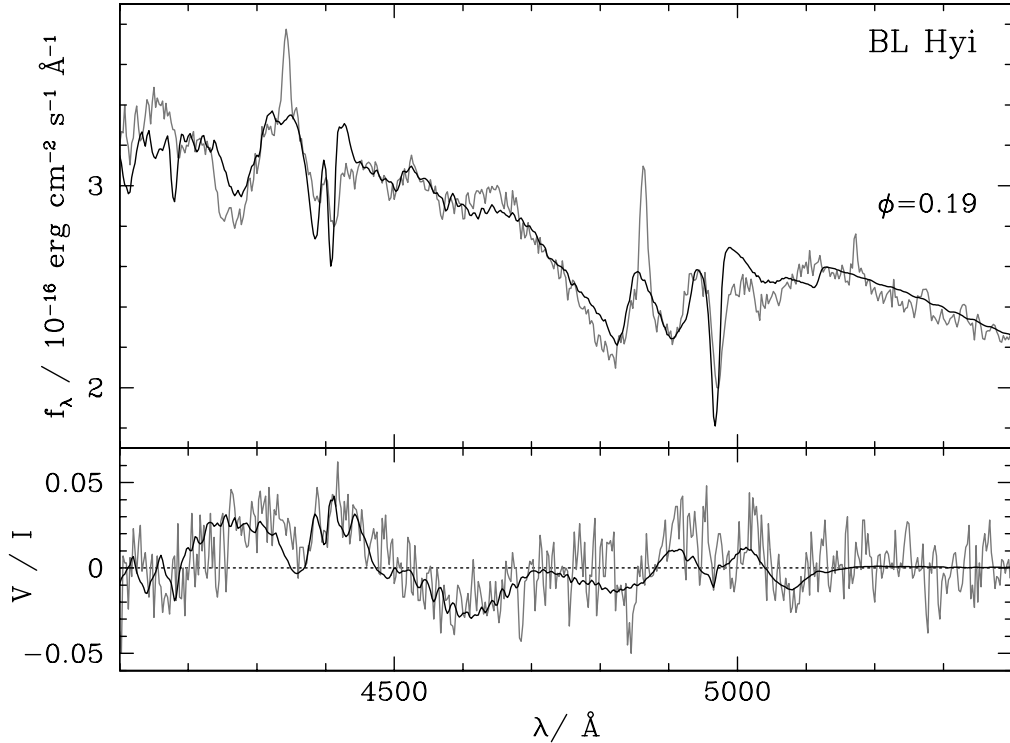


Figure 2. Flux (top) and circular polarization (bottom) spectra of BL Hyi at rotational phase $\Phi = 0.19$. The synthetic spectra for the best-fit model (black line) consisting of a truncated multipole expansion up to order $l = 3$ are shown superimposed on the observed spectra (grey curve).

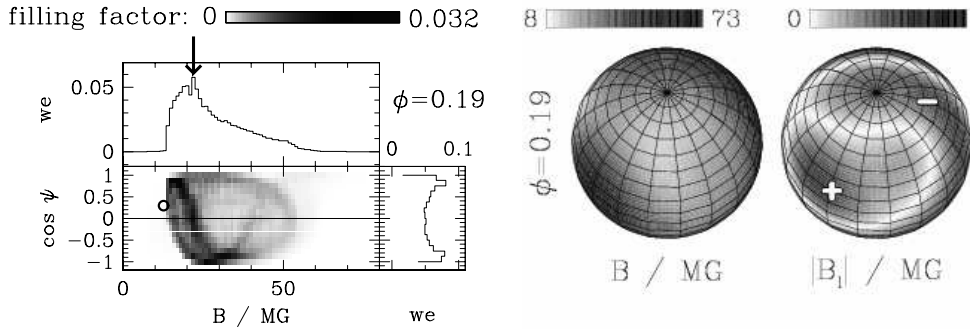


Figure 3. Left: Frequency distribution of the magnetic field strength $|\vec{B}|$ and the viewing direction cosine of \vec{B} , $\cos \psi$. Right: Distribution of $|\vec{B}|$ and its longitudinal component B_l on the white dwarf in BL Hyi at rotational phase $\Phi = 0.19$. The vertical arrow in the left diagram marks the average effective photospheric field strength, $B_{\text{eff}} = 22 \text{ MG}$; the open circle depicts the halo field strength, $B_{\text{halo}} = 12 \text{ MG}$ (Schwope et al. 1995) with the location of the main accretion pole derived by Piirola et al. (1987).

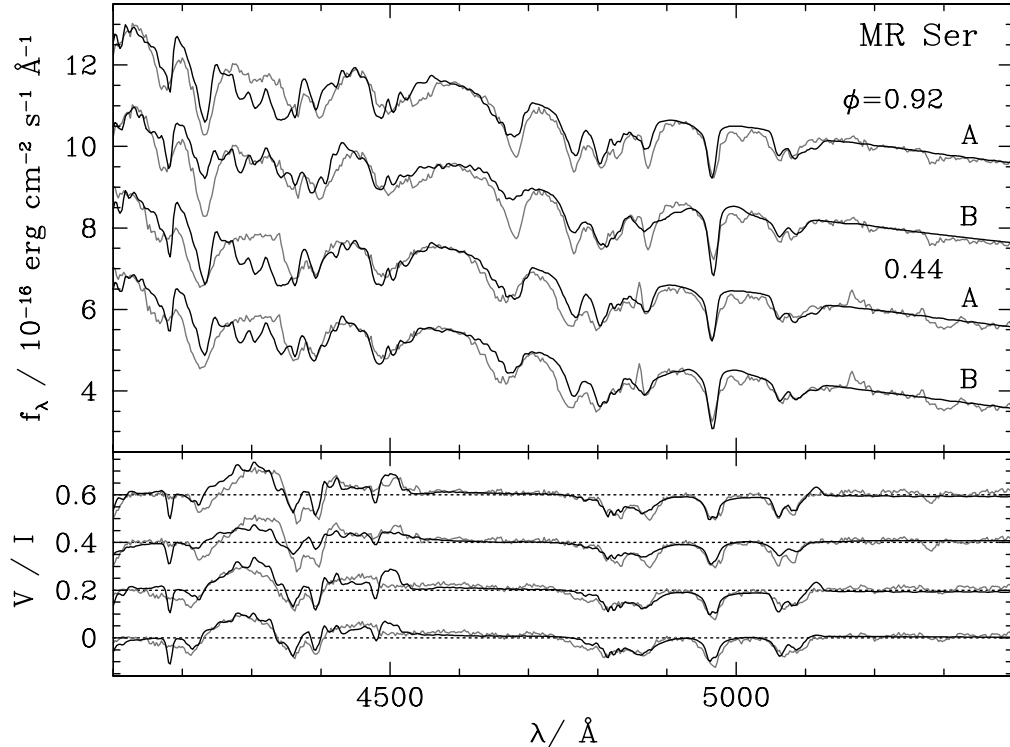


Figure 4. Flux (*top*) and circular polarization (*bottom*) spectra of MR Ser at $\Phi = 0.92$ (faint phase) and $\Phi = 0.44$ (bright phase). For each phase the observed spectra (grey curves) are compared with two different models (black lines): (A) an offset dipole field, (B) a multipole expansion up to order $l = 3$. For clarity, the upper three spectra have been offset by 2, 4, and 6 flux units, and the polarization spectra by 0.2, 0.4, and 0.6 units, respectively.

larimetry of the magnetic cataclysmic variables BL Hyi and MR Ser. Data were taken in multi-object spectropolarimetric mode (PMOS) with FORS1 at the ESO VLT while both systems were in low states of accretion.

During data reduction instrumental polarization effects and linear polarization cross-talk have been taken into account by computing circular polarization (V/I) spectra from two subsequent exposures taken with retarder plate position angles $\phi = -45^\circ$ and $\phi = +45^\circ$. Atmospheric absorption losses have been corrected for using the spectra of simultaneously observed field stars. Wavelength-dependent flux losses due to varying seeing conditions have been compensated for by normalizing the flux spectra to a mean continuum level.

4. Results

4.1. BL Hyi

Spectropolarimetric observations of BL Hyi have been obtained on 4 December 1999 and cover one complete rotational period of the accreting white dwarf. From the data we have extracted flux and polarization spectra at five rotational

phases according to the ephemeris of Wolff et al. (1999). In Fig. 2 we show a comparison of our observations and the best fit model near the maximum of the bright phase ($\Phi = 0.19$), i.e. when the main accretion region is visible. The observed Zeeman features of the Balmer lines $H\alpha$, $H\beta$, and $H\gamma$ vary significantly with rotational phase and require a multipole expansion up to order $l = 3$ to describe the field topology (Fig. 3).

Our best fit solution reveals a complex field topology but is consistent with the main characteristics like the average effective photospheric field strength, $B_{\text{eff}} = 22$ MG, and the halo field strength, $B_{\text{halo}} = 12$ MG, derived from intensity spectra alone (Schwope et al. 1995).

4.2. MR Ser

On 23 May and 24 May 2004 we have obtained 5.7 hours of spectropolarimetry of MR Ser equivalent to three rotational periods. The extracted flux and polarization spectra have been grouped into six rotational phase bins according to the ephemeris given by Schwope et al. (1993). In Fig. 4 we show the faint phase ($\Phi = 0.92$) and the bright phase ($\Phi = 0.44$) spectra, respectively. We have obtained two possible solutions for the field topology (Figs. 5 and 6). The first one consists of a dipole with $B = 53$ MG which has been offset along the dipole axis by 0.19 white dwarf radii. The second model is a truncated multipole expansion up to order $l = 3$ and provides a slightly better fit to the data. Again, our more complex field topologies match well the global field characteristics ($B_{\text{eff}} = 28$ MG, $B_{\text{halo}} = 24$ MG) observed previously (Schwope et al. 1993).

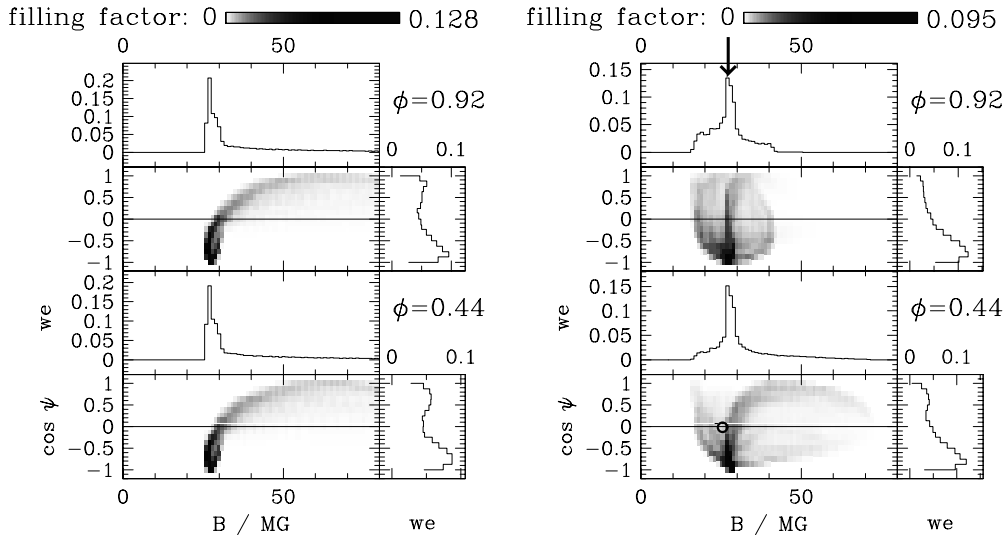


Figure 5. Frequency distribution of the magnetic field strength $|\vec{B}|$ and the viewing direction cosine of \vec{B} , $\cos \psi$, on the white dwarf in MR Ser at rotational phases $\Phi = 0.92$ and $\Phi = 0.44$, respectively, derived for the two models: (left) offset dipole, (right) truncated multipole. The vertical arrow in the right diagram marks the average effective photospheric field strength, $B_{\text{eff}} = 28$ MG; the open circle depicts the halo field strength, $B_{\text{halo}} = 24$ MG, reported by Schwope et al. (1993).

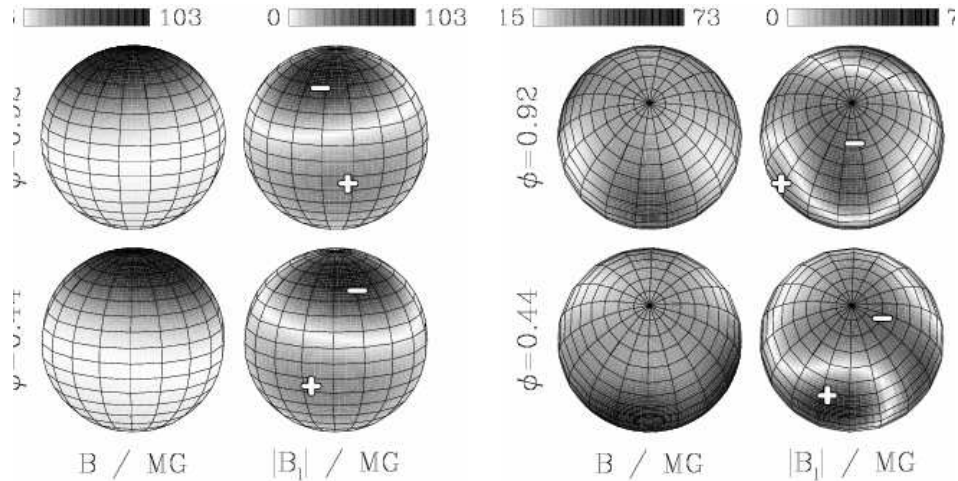


Figure 6. Distribution of the total magnetic field strength B and its longitudinal component B_l on the white dwarf in MR Ser at rotational phases $\Phi = 0.92$ and $\Phi = 0.44$, respectively, derived for the two models: (left) offset dipole, (right) truncated multipole.

5. Conclusions

The Zeeman tomographical analysis of phase-resolved spectropolarimetry provides for the first time detailed information about the range of field strengths and the field topology of accreting white dwarfs. For both systems discussed here we find that at least multipole expansions up to order $l = 3$ are required to describe the field topologies. Remaining residuals indicate that the field topologies might even be more complex.

Acknowledgments. Based on observations collected at the European Southern Observatory, Chile under program numbers 64.P-0150(C) and 073.D-0322(B).

References

Beuermann, K. 1998, in *High Energy Astron. & Astrophys.*, Tata Inst. of Fund. Res., 100
 Cumming, A. 2002, MNRAS, 333, 589
 Euchner, F., Jordan, S., Beuermann, K., et al. 2002, A&A, 390, 633
 Gänsicke, B.T., Euchner, F., & Jordan, S. 2002, A&A, 394, 957
 Liebert, J., Bergeron, P., & Holberg, J. B. 2003, AJ, 125, 348
 Pirola, V., Reiz, A., & Coyne, G.V. 1987, A&A, 185, 189
 Romani, R. 1990, Nat, 347, 741
 Schmidt, G. D., Harris, H.C., Liebert, J., et al. 2003, AJ, 595, 1101
 Schwone, A. D., Beuermann, K., Jordan, S., & Thomas, H.-C., 1993, A&A, 278, 487
 Schwone, A. D., Beuermann, K., & Jordan, S. 1995, A&A, 301, 447
 Wickramasinghe, D.T., Ferrario, L. 2000, PASP, 112, 873
 Wolff, M. T., Wood, K. S., Imamura, J. N., et al. 1999, ApJ, 526, 435